# Self-Assembly Evolution of Metal-Free Naphthalocyanine Molecules on Ag(111) at Sub-Monolayer Coverage

**Article** *in* The Journal of Physical Chemistry C · March 2019

DOI: 10.1021/acs.jpcc.9b00095



**8 authors**, including:

Rongting Wu
Yale University
**17** PUBLICATIONS **980** CITATIONS
SEE PROFILE

Linghao Yan
Aalto University
**18** PUBLICATIONS **84** CITATIONS
SEE PROFILE

Deliang Bao
Vanderbilt University
**32** PUBLICATIONS **204** CITATIONS
SEE PROFILE

Junhai Ren
Tsinghua University
**9** PUBLICATIONS **27** CITATIONS
SEE PROFILE

THE JOURNAL OF PHYSICAL CHEMISTRY C

Article

Cite This: J. Phys. Chem. C 2019, 123, 7202−7208

pubs.acs.org/JPCC

# Self-Assembly Evolution of Metal-Free Naphthalocyanine Molecules on Ag(111) at the Submonolayer Coverage

Rongting Wu,[†,⊥] Linghao Yan,[†] De-Liang Bao,[†] Junhai Ren,[†] Shixuan Du,[†,§] Yeliang Wang,*[,†,‡,∥] Qing Huan,*[,†,§] and Hong-Jun Gao[†,§,∥]

[†]Institute of Physics and University of Chinese Academy of Sciences, Chinese Academy of Sciences, Beijing 100190, China

[‡]School of Information and Electronics, Beijing Institute of Technology, Beijing 100081, China

[§]Songshan Lake Materials Laboratory, Dongguan, Guangdong 523808, China

[∥]CAS Center for Excellence in Topological Quantum Computation, Beijing 100049, China

**ABSTRACT:** Structures of self-assembled films play essential roles in the performance of potential organic molecular electronics; therefore, detailed knowledge of molecular adsorption and structural evolution is fundamental for the implementation of molecular electronics. Here, we systematically investigated the initial adsorption and structure evolution of metal-free naphthalocyanine ($H_2Nc$) on the Ag(111) surface from dimers to ordered self-assembled structures in the submonolayer range. $H_2Nc$ molecules deposited on Ag(111) at 100 K accumulate into clusters dominated by dimers. Subsequent sample annealing induces the emergence of two ordered self-assembled structures, denoted by $S_I$ and $S_{II}$. Molecule-resolved scanning tunneling microscopy images confirm that structure $S_I$ is more stable with six rotation domains lying in two chiralities. Deviations of the lattice parameters from a threefold symmetry indicate non-neglectable intermolecular interactions in self-assembled patterns. Combined with density functional theory calculations, orientations of the two inner hydrogens of $H_2Nc$ in the self-assembled film are revealed.

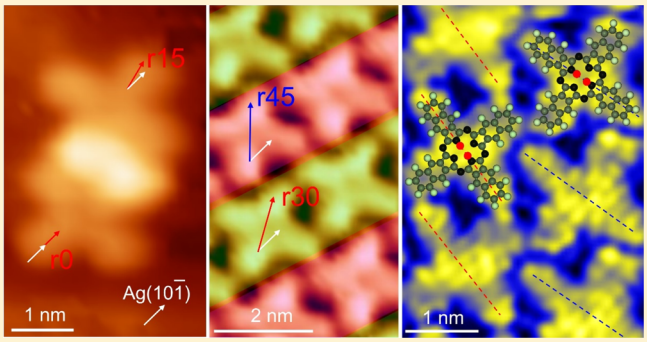


## INTRODUCTION

Organic functional molecules have been investigated extensively over the past decades because of their potential applications in electronic and optical devices, for instance, solar cells,[1,2] switches,[3,4] and light-emitting diodes.[5,6] The intermolecular and molecule−substrate interactions play dominant roles in the performance of these devices. Therefore, detailed knowledge about molecular adsorption and structural evolution is essential. Among organic functional molecules, phthalocyanines (Pcs) and their derivatives have attracted great interest caused by their fascinating physical properties[7−11] arising from the delocalized $\pi$-electronic structures. Plenty of studies about Pcs including the adsorption,[12−14] electronic properties,[7−9,15] and structure formations[12,13,16] have been reported.

Naphthalocyanine ($H_2Nc$), an important class of Pc derivatives with extended $\pi$-electronic system, reveals superior optical and electronic properties.[10,11,17−22] Initial investigations about the $H_2Nc$ molecules on surfaces are mainly focused on graphite[23,24] and insulators.[25,26] Recently, $H_2Nc$s on metallic substrates such as Au(100),[27] Au(111),[28,29] and Ag(111)[30,31] have been investigated. Among these studies, the self-assembled structures of densely packed phases such as domain orientations[27,28] and underlying mechanical strains[30] have been studied. However, the initial growth stage, especially the structure evolution process from a single molecule to the submonolayer ordered pattern, has been barely checked. This process is essential to understand the adsorption mechanism and structure evolution and control corresponding physical properties.

Here, we investigate the initial adsorption and structure evolution of metal-free $H_2Nc$ on a Ag(111) surface. A submonolayer coverage from dimers to ordered self-assembled structures has been studied. $H_2Nc$ clusters formed at low sample temperature are systematically investigated, where dimers are revealed as the dominant form in the initial adsorption stage. Structural transformations are induced by the subsequent sample annealing: two kinds of ordered self-assembled structures were observed, namely, configurations $S_I$ and $S_{II}$. With submolecular-resolution scanning tunneling microscopy (STM) images, we found that configuration $S_I$ is dominant on this stage and has totally six rotation domains lying in two chiralities. The lowest unoccupied molecular orbital (LUMO) of $H_2Nc$ molecules is successfully resolved, and the exact orientations of the inner two hydrogen atoms in

Received: January 4, 2019
Revised: February 20, 2019
Published: March 5, 2019






DOI: 10.1021/acs.jpcc.9b00095
J. Phys. Chem. C 2019, 123, 7202−7208

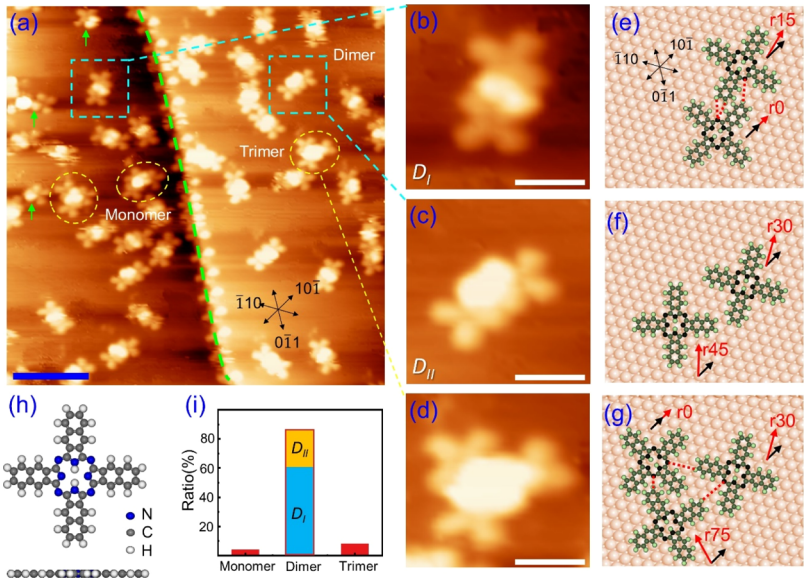


**Figure 1.** Initial growth stage of $H_2Nc$ molecules on Ag(111). (a) STM morphology of 0.24 ML $H_2Nc$ molecules on the Ag(111) surface, with the substrate kept at 100 K during $H_2Nc$ deposition (scale bar: 7 nm). (b) Zoom-in image of dimer configuration $D_I$ with two parallel lobes approaching each other. (c) Zoom-in image of dimer configuration $D_{II}$ with two perpendicular lobes approaching each other. (d) Zoom-in image of trimer configuration (scale bars in b, c, d: 2 nm). (e–g) Atomic model of the dimer $D_I$, dimer $D_{II}$, and trimer configurations on the Ag(111) surface. (h) Top-view and side-view model of the $H_2Nc$ molecule. (i) Statistic distribution of molecules in monomer, dimer, and trimer configurations.

an individual $H_2Nc$ molecule are unveiled in the self-assembled film.

## METHODS

**Experiments.** All experiments were carried out in a homemade ultrahigh vacuum (UHV) variable temperature scanning tunneling microscope[32] with the base pressure better than $2.0 \times 10^{-10}$ Torr. A single-crystal Ag(111) (roughness < 0.03 $\mu$m, orientation accuracy < 0.1°, MaTeck Company) was prepared in vacuum by repeated cycles of $Ne^+$ sputtering and subsequent annealing at 770 K until a clean surface was confirmed by STM imaging.[33] Naphthalocyanine ($H_2Nc$; Aldrich 95%+) in powder form was purified by the sublimation process with a homemade Knudsen Cell (K-cell) evaporator in high vacuum for 3 days, followed by degassing at 640 K for 2 h under UHV conditions. $H_2Nc$ was evaporated at 610 K with the Ag(111) substrate kept at 100 K. The evaporation rate is about 0.013 ML/min. A monolayer (ML) is defined as the amount of deposited $H_2Nc$ that entirely covers the substrate surface.[30] Electrochemically etched tungsten tips were used as STM tips, and they were further cleaned by several cycles of $Ne^+$ sputtering and annealing in UHV and checked by STM imaging. All the STM images were taken in constant-current mode at 100 K, with the bias applied to the sample.

**Calculations.** Density functional theory (DFT) calculations were performed using the VASP code[34,35] with the projector-augmented wave method.[36] The Perdew–Burke–Ernzerhof[37] version of the generalized gradient approximation[38] was used. The plane-wave cutoff was 400 eV. The unit cell is a 30 Å × 30 Å × 15 Å box containing an isolated $H_2Nc$ molecule in the center. All atoms were relaxed until the forces between atoms were smaller than 0.01 eV/Å in the structural relaxation. The Brillouin zone was sampled with only the Γ-point.

## RESULTS AND DISCUSSION

The $H_2Nc$ molecule comprises a planar geometry with a van der Waals diameter of around 2 nm, as schematized in Figure 1h. Because of the weak interaction between the $H_2Nc$ molecule and the Ag(111) surface, submonolayer $H_2Nc$ molecules cannot be observed by a scanning tunneling microscope, while the sample temperature is kept at room temperature.[30] Thus, to investigate the initial growth stage, we deposit $H_2Nc$ molecules onto the Ag(111) substrate at a low sample temperature of 100 K. The typical morphologies after deposition are shown in Figure 1a. At a coverage of 0.24 ML, most $H_2Nc$ molecules are scattered over the terraces. The step edge is fully occupied, as marked by the green dashed line, which was confirmed by extensive STM images taken in different areas. This agrees with the well-known terrace–step–kink model[39] for the thin film growth, and the step edge is superior adsorption site to terrace.

Very interestingly, we find that most of the molecules on terrace accumulate to form clusters with different sizes. Dimers are dominant in the initial stage, while few monomers and trimers also exist, as highlighted by green arrows and yellow dashed circles in Figure 1a. Further analysis on the dimers revealed that all dimers come from two configurations, namely, configuration $D_I$ with two parallel lobes approaching each other and configuration $D_{II}$ with two neighboring perpendicular lobes. The high-resolution STM images of these two configurations are presented in Figure 1b,c, respectively. Notably, the two adjacent lobes are much brighter than other lobes in both configurations. This brightness difference may result from two possible reasons. First, the neighbor lobes rise a little to accommodate larger molecule–molecule interactions. Second, some adatoms exist in between to attain a more stable adsorption configuration. Further analysis about the intermolecular distance in these two dimers indicates that there is no space for the adatoms in configuration $D_I$, whereas they may exist in configuration $D_{II}$. Figure 1d exhibits the high-



DOI: 10.1021/acs.jpcc.9b00095
J. Phys. Chem. C 2019, 123, 7202–7208

resolution STM image of one typical trimer. Similarly, the three adjacent lobes are much brighter than other lobes.

By comparing the atomic-resolved STM images of the Ag(111) substrate and the orientations of $H_2Nc$ molecules, schematic models of the above-mentioned three configurations are derived, as shown in Figure 1e–g. The highly packed symmetric orientations of the Ag(111) surface are denoted by the black arrows, whereas the orientations of $H_2Nc$ lobes are highlighted by red arrows. Statistic distribution of $H_2Nc$ molecules in different-sized clusters is presented in Figure 1i, from where we find that ~85.9% of the molecules accumulate into dimers and ~70.9% of the dimers adopt configuration $D_I$. The ratios of the molecules in the monomers and trimers are only ~4.7 and ~9.4%, respectively.

The minor monomers on the surface after deposition are quite interesting. One could imagine that most $H_2Nc$ molecules deposited on the surface possess large enough kinetic energy to overcome the diffusion barrier on the terrace and move freely at 100 K. This situation changed once two molecules meet and form a dimer. The dominant $H_2Nc$ dimers on the initial stage indicate a net attractive interaction between $H_2Nc$ molecules. It is noteworthy that all monomers adsorb to some small white clusters (Figure 1a), as highlighted by green arrows. These clusters would provide additional adsorption energy to anchor the $H_2Nc$ molecules.

By careful analysis on the most stable dimer configuration $D_I$, we find that the two molecules assemble in a way with the lobe of one molecule close to the center of the other molecules. In this status, the hydrogen bonds form between the nitrogen atom in the lobe shoulders and the hydrogen atom in the lobe terminals, as highlighted by the red dashed line in Figure 1e, which should play an important role in the net attractive interaction.

In order to investigate the thermal stability of the initial adsorption configurations of $H_2Nc$ molecules on the Ag(111) surface, we anneal the sample up to 200 K for 1 h and then cool down to 100 K for STM measurements. Interestingly, after annealing at 200 K, the morphology of the $H_2Nc$ molecular film on Ag(111) changed dramatically, and some ordered self-assembled structures appear. Figure 2a presents one typical ordered self-assembled structure, namely, $S_I$, where the crosslike $H_2Nc$ molecules pack together with the two molecular crystal lattice directions intersected by 75°, as highlighted by the two black lines. This self-assembly differs from the densely packed structures in previous reports, where the packed angle is around 90°.[30] Within this self-assembled domain, some dislocation line defects could be observed as marked by the red dashed line. Areas covered with disordered $H_2Nc$ molecules also exist, with the boundary between ordered and disordered areas highlighted by the yellow dashed line.

Figure 2c shows the high-resolved STM image of the ordered structure within the blue rectangle in Figure 2a. Detailed analysis reveals that this kind of ordered self-assembled structure is constructed by $H_2Nc$ molecules with two different configurations arrayed in alternate rows as highlighted in red and yellow. By comparing the orientations of $H_2Nc$ molecules and the atomic-resolution STM images of the Ag(111) substrate, we found that the $H_2Nc$ molecules in these two configurations rotate 45° and 30° in anticlockwise direction with respect to the substrate atomic orientation, and here we name these two configurations as r45 and r30, respectively.

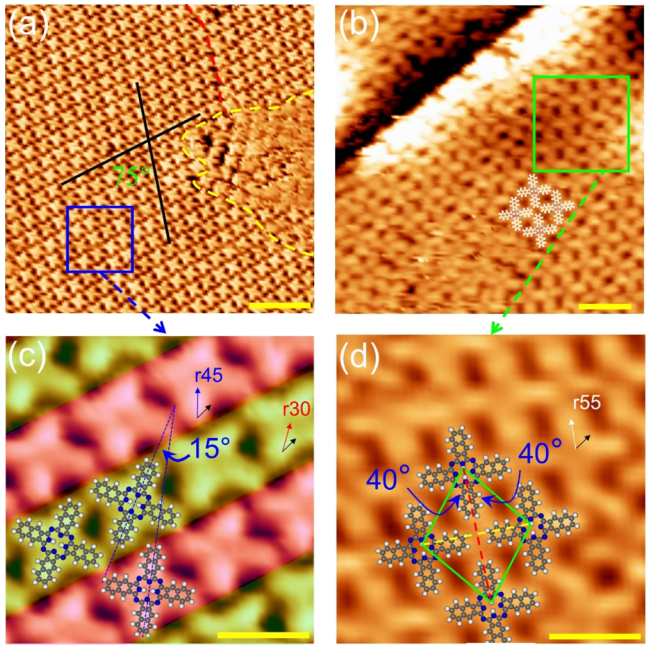


**Figure 2.** Morphology of the submonolayer $H_2Nc$ molecules on Ag(111) after sample annealing. (a,b) Ordered self-assembled configurations $S_I$ and $S_{II}$ after sample annealing at 200 K (scale bar: 7 and 3 nm, respectively). (c,d) Zoom-in STM images of the self-assembled configurations $S_I$ and $S_{II}$ (scale bar: 2 nm).

Another typical ordered self-assembled structure $S_{II}$ is shown in Figure 2b, where all molecules employ the same configuration and pack together in a loose manner forming a rectangle lattice. In contrast to the large domain size of structure $S_I$, this new structure $S_{II}$ only locally exists in some minor domains on the surface, which implies that it is less stable than structure $S_I$.

Figure 2d shows the high-resolved STM image of structure $S_{II}$ within the green square in Figure 2b, where $H_2Nc$ molecules pack together with the adjacent lobes pointing to each other. Furthermore, the unit cell of this structure as highlighted by the green line is a rhombus with the interior angle being 80°, which indicates that the $H_2Nc$ molecules pack a little denser in lateral direction (yellow dashed line) than in vertical direction (red dashed line). The orientation of the $H_2Nc$ molecule in this structure is 55° anticlockwise from the highly packed orientation of the substrate..

Because structure $S_I$ dominates on the annealed sample surface, systematic investigations of this ordered self-assembled structure are carried out. Detailed studies on the surface reveal that there are totally six different domains for structure $S_I$, as the high-resolved STM images presented in Figure 3. The $H_2Nc$ molecules are typically resolved as crosses with four bright lobes and a dark center, as highlighted by dashed crosses in different colors. All molecules pack together forming alternative arrays with different molecular orientations. The orientations of molecular arrays in one domain are the same, whereas they are different from domain to domain; therefore, we could distinguish six domains by the molecular array orientations. Here, we name the domain with a horizontal molecular array as R0 and name domains with molecular arrays rotated by 30°, 60°, 90°, 120°, and 150° from the horizontal orientation in anticlockwise direction as R30, R60, R90, R120, and R150, respectively. The blue and green rhomboids



DOI: 10.1021/acs.jpcc.9b00095
J. Phys. Chem. C 2019, 123, 7202−7208

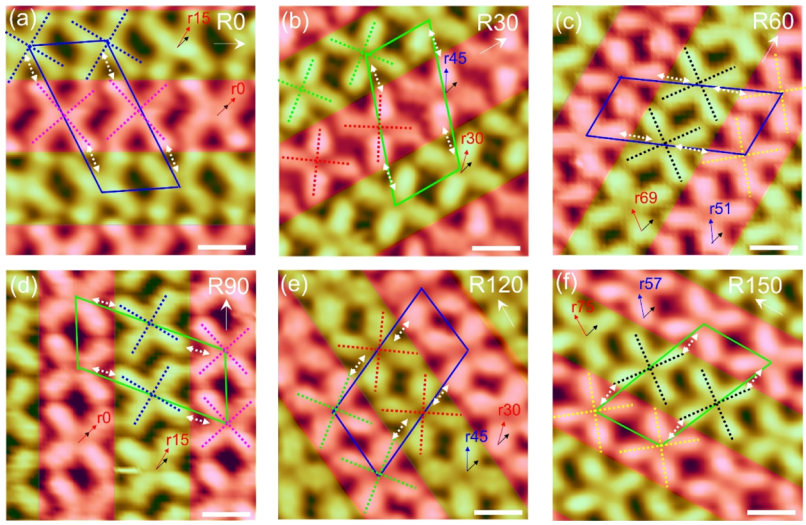


**Figure 3.** High-resolution STM images show the self-assembled configuration $S_I$ of $H_2Nc$ molecules on the Ag(111) surface. Six different domains are presented as R0, R30, R60, R90, R120, and R150 in (a–f), respectively. The red and yellow colors highlight the self-assembled orientation, the blue and green rhomboids identify the corresponding unit cells, and the crosses represent the orientations of each single molecule. The scanning parameters are −2.5 V, 0.1 nA in (a), −1.0 V, 0.1 nA in (b), −2.0 V, 0.1 nA in (c), −2.75 V, 0.1 nA in (d), −1.7 V, 0.1 nA in (e), and −2.2 V, 0.1 nA in (f), respectively (scale bar: 1 nm).

**Table 1. Geometric Parameter of the Six Self-Assembled $H_2Nc$ Molecular Domains Observed in the Experiment**[a]

| Structure | R0 | R30 | R60 | R90 | R120 | R150 |
|---|---|---|---|---|---|---|
| A (Å) | 19.7±0.5 | 19.1±0.5 | 17.9±0.5 | 18.2±0.5 | 19.2±0.5 | 19.4±0.5 |
| B(Å) | 37.9±0.9 | 37.4±0.9 | 41.1±0.9 | 38.7±0.9 | 37.5±0.9 | 36.2±0.9 |
| Φ(°) | 64±2 | 72±2 | 68±2 | 68±2 | 71±2 | 65±2 |
| Density (1/nm$^2$) | 0.298±0.019 | 0.294±0.019 | 0.293±0.02 | 0.306±0.022 | 0.293±0.02 | 0.314±0.024 |
| Coverage (1/ Layer) | 0.85 | 0.84 | 0.84 | 0.88 | 0.84 | 0.90 |
| Matrix Notation | $\begin{bmatrix}14 & 3\\ 5 & 8\end{bmatrix}$ | $\begin{bmatrix}13 & 0\\ 1 & 7\end{bmatrix}$ | $\begin{bmatrix}13 & 15\\ -2 & 5\end{bmatrix}$ | $\begin{bmatrix}14 & 12\\ -5 & 2\end{bmatrix}$ | $\begin{bmatrix}8 & 3\\ -2 & 12\end{bmatrix}$ | $\begin{bmatrix}1 & 13\\ 7 & 6\end{bmatrix}$ |
| Unit Cell |  |  |  |  |  |  |

[a]The matrix notation (orange background) indicates the closest commensurate structure to the corresponding unit cell.

highlight the unit cell in each self-assembled domain. After detailed analysis of the six domains, we find that they lie in two supramolecular chiralities, with domains R0, R60, and R120 sharing one chirality and the other three domains sharing another chirality, as highlighted by blue and green rhomboids. To distinguish each molecule in the domains, we define the configuration of a single molecule by the orientation of its one lobe with respect to the Ag(111) highly packed direction, as marked by r0, r15, r30, r45, r60, and r75 in each panel.

Apparently, in each unit cell, there are two molecules employing different configurations, which suggest that these configurations are energetically similar. The alternative arrangement of these two configurations in one domain, rather than two domains with homogeneous configuration, indicates an attractive force between these two neighboring molecules. Detailed analysis of the distance between the adjacent $H_2Nc$ molecules shows that one molecular lobe is particularly close to the center of the neighboring molecule, as highlighted by the white dashed double arrows in Figure 3. In accordance with the dominant dimer configuration $D_I$, we tentatively proposed that the hydrogen bonds, which formed between the hydrogen atoms on the lobe terminal and the nitrogen atom in the center of the neighboring molecule, produce the attractive force and enable this ordered structure.

With extensive molecular-resolved STM images, we accurately measured the lattice parameters of the unit cells in each domain as shown in Table 1. Because the Ag(111) substrate is threefold symmetric, the self-assembled $H_2Nc$ molecular domains within the same chirality are supposed to be threefold symmetric. Interestingly, after careful analysis about the lattice constant and intersection angle of different unit cells, we find quite large deviations among the three domains possessing the same chirality, as shown in the first three rows in Table 1. These deviations from the ideal threefold symmetry were reported in the ML $H_2Nc$ self-assembled film on Ag(111),[30] which indicates that for $H_2Nc$ on the Ag(111) system, the interaction between molecules plays a non-negligible effect in the self-assembly process. With detailed lattice parameters of each unit cell, the density and coverage of the $H_2Nc$ molecules in different self-assembled



DOI: 10.1021/acs.jpcc.9b00095
J. Phys. Chem. C 2019, 123, 7202−7208

domains are calculated as shown in Table 1. The density ranges from 0.29 to 0.31 molecules per square nanometers, which lead to a coverage of 0.84 ML to 0.9 ML. Here, one ML corresponds to the densely packed self-assembled film in the previous report.[30] The matrix and the unit cell for the six self-assembled domains are illustrated in Table 1 with light orange background.

Recently, the two hydrogen atoms in the inner cavity of $H_2Nc$ molecules have attracted more attention because of their potential application in molecular switches.[26] While most of the former work research on a single molecule or clusters with few molecules, properties about these two hydrogen atoms in ordered self-assembled films are essential for integrating molecular switches to a large scale, yet related studies are rare. Here, with submolecular-resolution STM images, we carried out detailed investigations on the orientations of the two inner hydrogen atoms in the ordered self-assembled films. Figure 4a shows the high-resolution STM image taken at a bias of −0.3 V on the self-assembled domain R90, and some fine features in the crosslike morphology appear. Apparently, the four lobes within one molecule are no longer identical, with two opposite sharp lobes and two opposite blunt ends, as highlighted by the red and blue dashed lines.

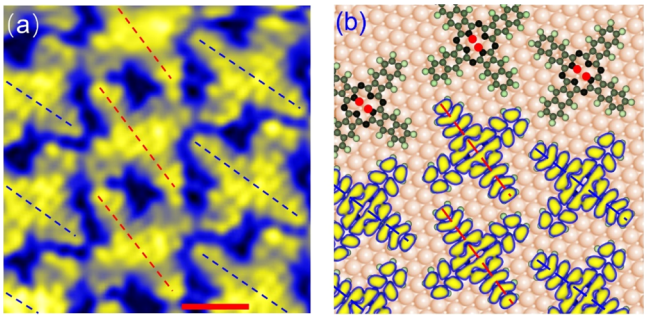


**Figure 4.** Orientations of two inner hydrogen atoms of an individual $H_2Nc$ molecule in the assembled film. (a) High-resolution STM image reveals the molecular orbital of the $H_2Nc$ molecule in the domain R90, and the red and blue dashed lines highlight the orientations of the two inner hydrogen atoms in the center cavity of an individual $H_2Nc$ molecule. The scanning parameter is −0.3 V, 0.1 nA (scale bar: 1 nm). (b) Atomic model and corresponding LUMO of the $H_2Nc$ molecule, which shows a good agreement with the STM image.

With detailed investigations on these new features, we find that the new STM morphology of $H_2Nc$ molecules matches quite well with the LUMO, as illustrated in the schematic model (Figure 4b), where some of the $H_2Nc$ molecules are superposed by their LUMO. The LUMO state is normally above the Fermi level, which should be captured in positive bias. The phenomenon that we captured this typical LUMO state at −0.3 V suggests considerable electron doping from the underneath Ag(111) substrate to the $H_2Nc$ molecules. With these fine features of the $H_2Nc$ molecular LUMO, we could distinguish that the inner two hydrogen atoms locate on the two sharp lobes, as highlighted by the red dots in Figure 4b. Detecting and understanding of the orientation of the two inner hydrogen atoms of the $H_2Nc$ molecules in the ordered self-assembled film are essential for potential applications of molecular logic devices.[26,40] By selectively switching the inner two hydrogen orientations in individual molecule, one could write in different information, that is, "bit", in the film, which deserves deeper studies in future.

## CONCLUSIONS

Initial adsorption and structure evolution of metal-free $H_2Nc$ on a Ag(111) surface from dimers to ordered self-assembled structures in the submonolayer range were systematically investigated by STM observations at variable sample temperatures. At 100 K, the initial deposited $H_2Nc$ molecular form clusters on the Ag(111) surface and dimers are observed as the dominant form at the initial stage. Subsequent annealing induced molecular adsorption structure transformation, and two kinds of ordered self-assembled structures were captured, namely, configurations $S_I$ and $S_{II}$, both of which are significantly different from the reported densely packed structures. When comparing these two ordered self-assembled structures, we found that configuration $S_I$ is more stable and dominant. Extensive molecular-resolved STM images disclose that structure $S_I$ has six rotation domains, which lie in two chiralities. Detailed lattice parameters of the six domains are obtained, and deviations of the lattice parameters from a threefold symmetry suggested non-neglectable intermolecular interactions in self-assembled patterns. With high-resolved STM image, we successfully captured the LUMO of $H_2Nc$ molecules at −0.3 V. Combined with DFT calculations, we reveal the exact orientations of two inner hydrogen atoms of an individual $H_2Nc$ molecule in the self-assembled film, which sets the stage for potential applications of molecular logic devices in future.

## AUTHOR INFORMATION

### Corresponding Authors

*E-mail: ylwang@iphy.ac.cn (Y.W.).
*E-mail: huanq@iphy.ac.cn (Q.H.).

### ORCID

Rongting Wu: 0000-0003-2254-2591
Linghao Yan: 0000-0002-4860-8096
De-Liang Bao: 0000-0002-5070-4765
Shixuan Du: 0000-0001-9323-1307
Yeliang Wang: 0000-0002-8896-0748
Hong-Jun Gao: 0000-0002-6766-0623

### Present Address

⊥Department of Applied Physics, Yale University, New Haven, CT 06520, U.S.A.

### Notes

The authors declare no competing financial interest.

## ACKNOWLEDGMENTS

This work was financially supported by the NSFC (nos. 61725107, 51572290, and 61390501), the National Key Research & Development Projects of China (nos. 2016YFA0202300 and 2018FYA0305800), Strategic Priority Research Program of the Chinese Academy of Sciences (no. XDB30000000), the CAS Key Technology Research and Development Team Project (GJJSTD20170006), and National Key Scientific Instrument and Equipment Development Project of China (nos. 2013YQ12034501 and 2013YQ12034503).



DOI: 10.1021/acs.jpcc.9b00095
J. Phys. Chem. C 2019, 123, 7202−7208

## REFERENCES


(1) Koeppe, R.; Sariciftci, N. S.; Troshin, P. A.; Lyubovskaya, R. N. Complexation of Pyrrolidinofullerenes and Zinc-Phthalocyanine in a Bilayer Organic Solar Cell Structure. *Appl. Phys. Lett.* **2005**, *87*, 244102.

(2) Koeppe, R.; Hoeglinger, D.; Troshin, P. A.; Lyubovskaya, R. N.; Razumov, V. F.; Sariciftci, N. S. Organic Solar Cells with Semitransparent Metal Back Contacts for Power Window Applications. *ChemSusChem* **2009**, *2*, 309−313.

(3) Gao, H. J.; Sohlberg, K.; Xue, Z. Q.; Chen, H. Y.; Hou, S. M.; Ma, L. P.; Fang, X. W.; Pang, S. J.; Pennycook, S. J. Reversible, Nanometer-Scale Conductance Transitions in an Organic Complex. *Phys. Rev. Lett.* **2000**, *84*, 1780−1783.

(4) Moresco, F.; Meyer, G.; Rieder, K.-H.; Tang, H.; Gourdon, A.; Joachim, C. Conformational Changes of Single Molecules Induced by Scanning Tunneling Microscopy Manipulation: A Route to Molecular Switching. *Phys. Rev. Lett.* **2001**, *86*, 672−675.

(5) Wang, S.; Liu, Y.; Huang, X.; Yu, G.; Zhu, D. Phthalocyanine Monolayer-Modified Gold Substrates as Efficient Anodes for Organic Light-Emitting Diodes. *J. Phys. Chem. B* **2003**, *107*, 12639−12642.

(6) Forrest, S. R. The Path to Ubiquitous and Low-Cost Organic Electronic Appliances on Plastic. *Nature* **2004**, *428*, 911.

(7) Hipps, K. W.; Barlow, D. E.; Mazur, U. Orbital Mediated Tunneling in Vanadyl Phthalocyanine Observed in Both Tunnel Diode and Stm Environments. *J. Phys. Chem. B* **2000**, *104*, 2444−2447.

(8) Barlow, D. E.; Hipps, K. W. A Scanning Tunneling Microscopy and Spectroscopy Study of Vanadyl Phthalocyanine on Au(111): the Effect of Oxygen Binding and Orbital Mediated Tunneling on the Apparent Corrugation. *J. Phys. Chem. B* **2000**, *104*, 5993−6000.

(9) Lu, X.; Hipps, K. W.; Wang, X. D.; Mazur, U. Scanning Tunneling Microscopy of Metal Phthalocyanines: d7and d9Cases. *J. Am. Chem. Soc.* **1996**, *118*, 7197−7202.

(10) Hanack, M.; Schneider, T.; Barthel, M.; Shirk, J. S.; Flom, S. R.; Pong, R. G. S. Indium Phthalocyanines and Naphthalocyanines for Optical Limiting. *Coord. Chem. Rev.* **2001**, *219-221*, 235−258.

(11) El-Khouly, M. E.; Gutiérrez, A. M.; Sastre-Santos, Á.; Fernández-Lázaro, F.; Fukuzumi, S. Light harvesting zinc naphthalocyanine-perylenediimide supramolecular dyads: long-lived charge-separated states in nonpolar media. *Phys. Chem. Chem. Phys.* **2012**, *14*, 3612−3621.

(12) Gopakumar, T. G.; Lackinger, M.; Hackert, M.; Müller, F.; Hietschold, M. Adsorption of Palladium Phthalocyanine on Graphite: STM and LEED Study. *J. Phys. Chem. B* **2004**, *108*, 7839−7843.

(13) Suto, K.; Yoshimoto, S.; Itaya, K. Two-Dimensional Self-Organization of Phthalocyanine and Porphyrin: Dependence on the Crystallographic Orientation of Au. *J. Am. Chem. Soc.* **2003**, *125*, 14976−14977.

(14) Nilson, K.; Åhlund, J.; Brena, B.; Göthelid, E.; Schiessling, J.; Mårtensson, N.; Puglia, C. Scanning Tunneling Microscopy Study of Metal-Free Phthalocyanine Monolayer Structures on Graphite. *J. Chem. Phys.* **2007**, *127*, 114702.

(15) Zhang, Y. Y.; Du, S. X.; Gao, H. J. Binding Configuration, Electronic Structure, and Magnetic Properties of Metal Phthalocyanines on a Au(111) Surface Studied with Ab Initio Calculations. *Phys. Rev. B: Condens. Matter Mater. Phys.* **2011**, *84*, 125446.

(16) Ogunrinde, A.; Hipps, K. W.; Scudiero, L. A Scanning Tunneling Microscopy Study of Self-Assembled Nickel(Ii) Octaethylporphyrin Deposited from Solutions on HOPG. *Langmuir* **2006**, *22*, 5697−5701.

(17) El-Khouly, M. E.; Moiseev, A. G.; van der Est, A.; Fukuzumi, S. Photoinduced Electron Transfer in Zinc Naphthalocyanine-Naphthalenediimide Supramolecular Dyads. *ChemPhysChem* **2012**, *13*, 1191−1198.

(18) El-Khouly, M. E.; El-Mohsnawy, E.; Fukuzumim, S. Solar energy conversion: From natural to artificial photosynthesis. *J. Photochem. Photobiol. C* **2017**, *31*, 36−83.

(19) Pandey, R.; Kerner, R. A.; Menke, S. M.; Holst, J.; Josyula, K. V. B.; Holmes, R. J. Tin Naphthalocyanine Complexes for Infrared Absorption in Organic Photovoltaic Cells. *Org. Electron.* **2013**, *14*, 804−808.

(20) Lim, B.; Margulis, G. Y.; Yum, J.-H.; Unger, E. L.; Hardin, B. E.; Grätzel, M.; McGehee, M. D.; Sellinger, A. Silicon-Naphthalo/Phthalocyanine-Hybrid Sensitizer for Efficient Red Response in Dye-Sensitized Solar Cells. *Org. Lett.* **2013**, *15*, 784−787.

(21) Kobayashi, N.; Nakajima, S.-i.; Ogata, H.; Fukuda, T. Synthesis, Spectroscopy, and Electrochemistry of Tetra-Tert-Butylated Tetraazaporphyrins, Phthalocyanines, Naphthalocyanines, and Anthracocyanines, Together with Molecular Orbital Calculations. *Chem.—Eur. J.* **2004**, *10*, 6294−6312.

(22) Esmail, A. M. S.; Staddon, C. R.; Beton, P. H. Naphthalocyanine Thin Films and Field Effect Transistors. *J. Phys. Chem. C* **2016**, *120*, 15338−15341.

(23) Gopakumar, T. G.; Müller, F.; Hietschold, M. Scanning Tunneling Microscopy and Scanning Tunneling Spectroscopy Studies of Planar and Nonplanar Naphthalocyanines on Graphite (0001). Part 1: Effect of Nonplanarity on the Adlayer Structure and Voltage-induced Flipping of Nonplanar Tin−Naphthalocyanine. *J. Phys. Chem. B* **2006**, *110*, 6051−6059.

(24) Gopakumar, T. G.; Müller, F.; Hietschold, M. Scanning Tunneling Microscopy and Scanning Tunneling Spectroscopy Studies of Planar and Nonplanar Naphthalocyanine on Graphite (0001). Part 2: Tip−Sample Distance-DependentI−VSpectroscopy. *J. Phys. Chem. B* **2006**, *110*, 6060−6065.

(25) Yanagi, H.; Kouzeki, T.; Ashida, M. Epitaxial Growth of Naphthalocyanine Thin Films Vacuum Deposited on Alkali Halides. *J. Appl. Phys.* **1993**, *73*, 3812−3819.

(26) Liljeroth, P.; Repp, J.; Meyer, G. Current-Induced Hydrogen Tautomerization and Conductance Switching of Naphthalocyanine Molecules. *Science* **2007**, *317*, 1203−1206.

(27) Mehring, P.; Beimborn, A.; Lühr, T.; Westphal, C. Metal-Free Naphthalocyanine Structures on Au(100) at Submonolayer Coverage. *J. Phys. Chem. C* **2012**, *116*, 12819−12823.

(28) Wiggins, B.; Hipps, K. W. Investigation of Metal Free Naphthalocyanine Vapor Deposited on Au(111). *J. Phys. Chem. C* **2014**, *118*, 4222−4230.

(29) Pham, T. A.; Song, F.; Stöhr, M. Supramolecular Self-Assembly of Metal-Free Naphthalocyanine on Au(111). *Phys. Chem. Chem. Phys.* **2014**, *16*, 8881−8885.

(30) Wu, R.; Yan, L.; Zhang, Y.; Ren, J.; Bao, D.; Zhang, H.; Wang, Y.; Du, S.; Huan, Q.; Gao, H.-J. Self-Assembled Patterns and Young's Modulus of Single-Layer Naphthalocyanine Molecules on Ag(111). *J. Phys. Chem. C* **2015**, *119*, 8208−8212.

(31) Yan, L.-H.; et al. Adsorption Behavior of Fe Atoms on a Naphthalocyanine Monolayer on Ag(111) Surface. *Chin. Phys. B* **2015**, *24*, 076802.

(32) Stipe, B. C.; Rezaei, M. A.; Ho, W. A Variable-Temperature Scanning Tunneling Microscope Capable of Single-Molecule Vibrational Spectroscopy. *Rev. Sci. Instrum.* **1999**, *70*, 137−143.

(33) Wu, R.; Ren, J.; Dong, L.; Wang, Y.; Huan, Q.; Gao, H. J. Quasi-Free-Standing Graphene Nano-Islands on Ag(110), Grown from Solid Carbon Source. *Appl. Phys. Lett.* **2017**, *110*, 213107.

(34) Vanderbilt, D. Soft Self-Consistent Pseudopotentials in a Generalized Eigenvalue Formalism. *Phys. Rev. B: Condens. Matter Mater. Phys.* **1990**, *41*, 7892−7895.

(35) Kresse, G.; Furthmüller, J. Efficient iterative schemes forab initiototal-energy calculations using a plane-wave basis set. *Phys. Rev. B: Condens. Matter Mater. Phys.* **1996**, *54*, 11169−11186.

(36) Kresse, G.; Joubert, D. From Ultrasoft Pseudopotentials to the Projector Augmented-Wave Method. *Phys. Rev. B: Condens. Matter Mater. Phys.* **1999**, *59*, 1758−1775.

(37) Perdew, J. P.; Burke, K.; Ernzerhof, M. Generalized Gradient Approximation Made Simple. *Phys. Rev. Lett.* **1996**, *77*, 3865−3868.

(38) Perdew, J. P.; Chevary, J. A.; Vosko, S. H.; Jackson, K. A.; Pederson, M. R.; Singh, D. J.; Fiolhais, C. Atoms, Molecules, Solids, and Surfaces: Applications of the Generalized Gradient Approximation for Exchange and Correlation. *Phys. Rev. B: Condens. Matter Mater. Phys.* **1992**, *46*, 6671−6687.




DOI: 10.1021/acs.jpcc.9b00095
J. Phys. Chem. C 2019, 123, 7202−7208

(39) Burton, W. K.; Cabrera, N.; Frank, F. C. The Growth of Crystals and the Equilibrium Structure of Their Surfaces. *Philos. Trans. Royal Soc. A* **1951**, *243*, 299−358.
(40) Li, C.; Wang, Z.; Lu, Y.; Liu, X.; Wang, L. Conformation-Based Signal Transfer and Processing at the Single-Molecule Level. *Nat. Nanotechnol.* **2017**, *12*, 1071.



DOI: 10.1021/acs.jpcc.9b00095
*J. Phys. Chem. C* 2019, 123, 7202−7208